Molecular Biology of the Cell
Vol. 17, 4257–4269, October 2006

A Golgi-localized Hexose Transporter Is Involved in Heterotrimeric G Protein-mediated Early Development in *Arabidopsis*[D] [V]

Helen X. Wang,* Ravisha R. Weerasinghe,* Tony D. Perdue,* Nihal G. Cakmakci,* J. Philip Taylor,* William F. Marzluff,*† and Alan M. Jones*‡

Departments of *Biology, ‡Pharmacology, and †Biochemistry and Biophysics, The University of North Carolina at Chapel Hill, Chapel Hill, NC 27599-3280

Submitted January 23, 2006; Revised July 3, 2006; Accepted July 12, 2006
Monitoring Editor: J. Silvio Gutkind

Signal transduction involving heterotrimeric G proteins is universal among fungi, animals, and plants. In plants and fungi, the best understood function for the G protein complex is its modulation of cell proliferation and one of several important signals that are known to modulate the rate at which these cells proliferate is D-glucose. *Arabidopsis thaliana* seedlings lacking the β subunit (AGB1) of the G protein complex have altered cell division in the hypocotyl and are D-glucose hypersensitive. With the aim to discover new elements in G protein signaling, we screened for gain-of-function suppressors of altered cell proliferation during early development in the *agb1-2* mutant background. One *agb1-2*-dependent suppressor, designated *sgb1-1*^{D} for suppressor of *G* protein *b*eta1 (*agb1-2*), restored to wild type the altered cell division in the hypocotyl and sugar hypersensitivity of the *agb1-2* mutant. Consistent with AGB1 localization, SGB1 is found at the highest steady-state level in tissues with active cell division, and this level increases in hypocotyls when grown on D-glucose and sucrose. SGB1 is shown here to be a Golgi-localized hexose transporter and acts genetically with *AGB1* in early seedling development.

INTRODUCTION

An evolutionarily ancient mechanism for sensing extracellular signals involves the heterotrimeric G proteins, composed of α, β, and γ subunits. Heterotrimeric G protein complexes link ligand perception via seven-transmembrane (7TM), G protein-coupled receptors (GPCRs) to downstream effectors. Genes that encode G protein signaling elements have been identified in amoebae, fungi, plants, and animals, but among all multicellular eukaryotes, plants have the simplest repertoire of G protein elements to date. Specifically, the *Arabidopsis* genome encodes a single canonical Gα and Gβ (AGB1) subunit and two Gγ subunits and a single regulator of G signaling (RGS1) protein (Jones and Assmann, 2004). There are as yet no plant GPCRs having confirmed ligands, although plants do have a limited set of predicted 7TM proteins (Moriyama and Jones, unpublished data). Similarly, there are few known downstream effectors that physically interact with either the plant Gα subunit or the Gβγ dimer. One example is a pirin protein (Lapik and Kaufman, 2003), known to serve as a transcriptional cofactor in humans, but with unknown function in *Arabidopsis*. Based on either genetic or biochemical tests, Gα effectors in plants also include phospholipase D (Mishra *et al*., 2006) and ion channels (Aharon *et al*., 1998; Wang *et al*., 2001). Recently, we reported that a plant interactor and putative effector to Gα is an outer membrane plastid protein designated THF1, and this protein together with Gα comprises part of a D-glucose signaling network (Huang *et al*., 2006).

In animals and yeast, heterotrimeric G proteins couple a diverse set of signals such as photons, ions, small molecules, sugars, peptides, and protein ligands (Jones and Assmann, 2004) to control a broad range of physiology (Csaszar and Abel, 2001; Rosenkilde *et al*., 2001; Rockman *et al*., 2002). Many GPCR ligands stimulate cell proliferation, and these pathways are co-opted in disease (Dhanasekaran *et al*., 1995; Radhika and Dhanasekaran, 2001). Twelve carcinomas have been linked to mutations in GPCRs, and two carcinomas have been associated with activating mutations in Gα subunits, suggesting a connection between G protein-coupled pathways and cancer and/or cell proliferation. Other mutations of Gα subunits also have transforming potential when tested in cultured cell lines. Virally encoded GPCRs can be essential for infectivity or neoplastic potential of the virus, as is the case for cytomegalovirus infection or Kaposi's sarcoma, respectively (Sadee *et al*., 2001).

In yeast, the role of the Gβγ (Ste4/Ste18) dimer in regulating cell proliferation is the best understood. The protein–protein interface between the three sets of effectors and Ste4 subunit becomes available after the yeast Gα subunit (GPA1) becomes activated. Ste4 binds three effectors that ultimately regulate gene transcription through a mitogen-activated protein kinase cascade leading to growth arrest (Dohlman, 2002). Sugar is an important signal that controls yeast cell proliferation and size (Vanoni *et al*., 2005), and the Gβγ dimer is required in most, but not all fungi.

In *Arabidopsis*, altered cell proliferation either from defective cell division and/or expansion control is the underlying

This article was published online ahead of print in *MBC in Press* (http://www.molbiolcell.org/cgi/doi/10.1091/mbc.E06–01–0046) on July 19, 2006.

[D] [V] The online version of this article contains supplemental material at *MBC Online* (http://www.molbiolcell.org).

Address correspondence to: Alan M. Jones (alan_jones@unc.edu).

cause for many of the phenotypes of tissues and organs lacking the β subunit of the heterotrimeric G protein complex (*agb1-2*) (Lease *et al*., 2001; Ullah *et al*., 2001, 2003; Chen *et al*., 2006a). For example, 2-d-old *agb1-2* etiolated hypocotyls have one-half the number of epidermal cells as wild-type hypocotyls (Ullah *et al*., 2003). Adult plants have altered morphology, conspicuously rounder leaves, larger rosettes, and short siliques, but they also have several other quantitative changes as well (see Figure 4 of Ullah *et al*., 2003). Auxin-induced lateral root initiation and high-sugar sensing are also aberrant in the *agb1-2* seedlings (Ullah *et al*., 2001, 2002, 2003; Chen *et al*., 2003; Chen and Jones, 2004). *agb1-2* single and *agb1-2 gpa1-4* double mutant seedlings grown on 6% D-glucose have a complex response. Seedlings lacking AGB1 are severely hypersensitive to D-glucose. Seedlings that are able to germinate on high glucose have greatly expanded epinastic leaves and increased anthocyanin content (Supplemental Figure S1, B and C).

Using a genetic approach, we sought components downstream of the G protein complex regulation of cell proliferation and possibly sugar signaling. We found a novel Golgi hexose transporter that suppresses some of the loss-of-function Gβ phenotypes, including the deficiency in hypocotyl development and the altered sugar sensitivity of young seedlings. The biological function of this transporter was previously unknown and its genetic interaction with Gβ represents the first involvement of the G protein pathway in sugar transport and the first signal transduction pathway between the Golgi and Gβγ dimer of G proteins in a plant cell.

MATERIALS AND METHODS

Screen for Dominant Extragenic Mutations That Suppress the agb1-2 Hypocotyl and Hook Phenotypes and Plasmid Rescue

agb1-2 was transformed with the activation tagging vector, pSK1015, by *Agrobacterium*-mediated transformation (Bechtold *et al*., 1993). The activation-tagging vector consisted of four CaMV 35S enhancers and *bar* gene as a selection maker as described by Weigel *et al*. (2000). T1 seeds were sterilized (2.5% NaOCl), stratified in H_2O for at least 2 d, and then sown on medium at a density of ~2000 seeds per Petri dish (100 × 15 mm) containing 1/2 Murashige and Skoog salts (MS), 1% sucrose, 0.5% phyto agar (Research Products International, St. Prospect, IL), pH 5.7, 200 mg/l Timentin. After a 2- to 4-h light pretreatment, seeds were incubated in the dark at 23°C for 60 h. Control plant seeds were placed on the same plates in a marked area for reference. In total, 2,000,000 seedlings were screen without selection for transformation. Because the transformation efficiency was ≈1%, we estimate that 20,000 seedlings contained the activation tag. Seedlings looking similar to Col-0 were selected as suppressor candidates. These plants were transferred into soil and grown at 23°C in long-day conditions (16 h of light and 8 h of dark). Plasmid rescue using HindIII-digested *SGB1-1*^{D} genomic DNA was carried out as described by Weigel *et al*. (2000).

Cloning, Reverse Transcription-Polymerase Chain Reaction (RT-PCR), and Sequencing

SGB1 mRNA (1488 base pairs) was predicted based on the TAIR database information for locus At1g79820 (http://www.arabidopsis.org/abrc). The promoter sequence was defined here as the upstream sequence of *SGB1* between the stop codon of the upstream locus, At1g79830, and start codon of At1g79820. All PCR reactions for cloning were conducted using high-fidelity Phusion DNA polymerase (Phusion, Espoo, Finland). The PCR products were verified by sequencing. The 14 plasmids generated for this study are listed in Supplemental Table S1 followed by a description of their construction. The primers used for cloning, genotyping, and sequencing are listed in Supplemental Table S1. The *SGB1* cDNA was PCR amplified using the first-strand cDNA and ligated into pENTR D-TOPO (Invitrogen, Carlsbad, CA). For fusion proteins, the *SGB1* promoter flanked by NotI in pHW106 was cut and inserted into pHW123 in the NotI site. The resulting plasmid was recombined with proper destination vectors to make pHW128, 129 and 130, as listed in Supplemental Table S3. The binary vectors were transformed into *Agrobacterium* strain GV3101 by electroporation. *Arabidopsis* plants were transformed using floral infiltration (Bechtold *et al*., 1993).

The cDNA sequence of *Arabidopsis SGB1* was optimized for yeast preferred codon for the first eight amino acids at the N terminus and the stop codon at C terminus (Supplemental Table S1). Yeast expression plasmids used in this study contained the ADH promoter for high-level constitutive expression. The 1.5-kilobase (kb) *SGB1* fragment from pHW116, digested with XmaI, was inserted into the yeast/*Escherichia coli* shuttle vector p416 ADH in the XmaI site (*CEN6 ARSH4 URA3*) (Mumberg *et al*., 1995). The vectors were either antisense (pHW117) or sense (pHW118). The vectors were transformed into yeast strains using TE/LiAc/PEG protocol (Clontech, Mountain View, CA). The transformed yeast were grown on synthetic medium (SD) with uracil dropout as the selection marker. The medium was supplemented with 2% glucose for all strains except 2% maltose for the mutant strain EBY.VW4000.

The oocyte expression vector pXFRM contains Sp6 promoter, 5′- and 3′-β-globin untranslated region regions for efficient translation in oocyte systems (Wang *et al*., 1999; Sànchez and Marzluff, 2002). The *SGB1* cDNA with restriction sites NcoI at 5′ and XmaI at 3′ end was PCR amplified. The PCR product was digested with NcoI and XmaI and inserted into the digested pXFRM vector; this generated pHW136 (*SGB1* sense in frame) and pHW139 (with a spontaneous mutation). To make pHW137 with *SGB1* antisense, *SGB1* fragment was cut with XmaI from pHW117 and inserted into XmaI-digested pXFRM vector.

mRNA levels were determined using a total of RNA isolated from various tissues plants by using RNAeasy plant mini kit (QIAGEN, Valencia, CA). RT PCR was performed using ThermoScrpt RT-PCR system (Invitrogen). First-strand cDNA synthesis was performed using a poly(dT) primer.

Bioinformatics and Cladistics

Unrooted phylogenetic trees (unrooted) were constructed using the GeneBee algorithm accessed at http://www.genebee.msu.su/services/hlp/phtree-hlp.html (Brodsky *et al*., 1992, 1995). Homologues used for constructions of the phylogenetic trees were chosen from BLAST results by using the full-length *Arabidopsis* SGB1 protein sequence against the *Arabidopsis* (cut-off at 4×10^{-16}), yeast (cut-off at 4.8×10^{-11}), and human genomes (cut-off at 8×10^{-11}). Topological models were generated using a topological algorithm to generate unrooted phylogenetic trees for *Arabidopsis* and yeast comparisons. A cluster model was used in the comparison to human glucose transporters. Organelle targeting probabilities were calculated using TargetP version 1.01 Server from http://www.cbs.dtu.dk/services/TargetP/(Nielsen *et al*., 1997; Olof *et al*., 2000), which generated the same data as in TAIR for At1g79820 (http://www.mitoz.bcs.uwa.edu.au/apmdb/Flatfile-Script.php?chrlocus=AT1G79820.1).

Microscopies

Confocal laser-scanning microscopy was performed on roots, leaves, and seedlings by using a Zeiss LSM510 confocal laser scanning microscope (Carl Zeiss, Thornwood, NY). Freshly prepared plant parts were placed on a glass slide in a drop of water and covered with a glass coverslip. All images were collected using a Zeiss PlanNeofluar 40× numerical aperture 1.3 oil immersion objective. Yellow fluorescent protein (YFP) was visualized using 514-nm excitation and a 530- to 560-nm bandpass emission filter. Green fluorescent protein (GFP) fluorescence was visualized using 488-nm excitation and either a 505- to 550-nm bandpass or a 505-nm longpass emission filter. Root tissues were stained in 10 μM rhodamine123 solution (dissolved in water) for 5 min at room temperature and washed with distilled water. Confocal images of rhodamine123 were collected using 543-nm excitation and a 560- to 615-nm bandpass emission filter. Roots were treated with MitoTracker Orange CMTMRos for 20 min, and images were collected using 543-nm excitation and a 560-nm long-pass emission filter.

Differential interference contrast (DIC) and fluorescent microscopies of hypocotyl epidermal cells was performed on an Olympus XI81 inverted scope platform (Olympus America, Mellville, NY) using Nomarski optics, and images captured with a Cascade II charge-coupled device (Roper, Scientific, Trenton, NJ) and analyzed using IPLab and NIH Image 1.61 software. Seedlings were grown for 2 d in the dark on 1/2 MS medium supplemented with 1% glucose and then cleared in chloral hydrate. Average cell length was made from five cells at each position using multiple hypocotyls.

The Col-0 transgenic seeds bearing with pHW138 (*35S*::SGB1-GFP) were germinated in the dark at 23°C on 1/2 MS medium with 1% sucrose. Six-day-old seedlings were stained with ice-cold 1 μM BODIPY 558/568 brefeldin-A (BFA) (Invitrogen) at room temperature for 20 min. The root hairs were observed using laser-scanning confocal microscopy. Root hairs had good penetration for BODIPY 558/568 BFA; however, the proper concentration of the dye and the age of the root hairs of a seedling are critical to avoid any effect of the de-esterified BFA, to obtain optimal penetration, and to avoid background fluorescence.

Assays

The histochemical staining method for β-glucuronidase (GUS) activity is described by Malamy and Benfey (1997). Briefly, except for 2-d-old seedlings, all samples for histochemical analysis in GUS solution were gently degassed for 5 min for plants. After staining overnight, the samples were washed three times and cleared in 75% ethanol, in which samples were also stored.

For yeast growth assays, three independent colonies of each transformed yeast strain were cultured overnight on a rotary shaker at 30°C until the stationary stage ($OD_{600} > 1.0$) in 5 ml of minimal medium (YNB supplemented with histidine, leucine, and methionine [uracil dropout], containing 2% glucose and 200 μg/ml Geneticin). The cultures were then diluted to OD_{600} ~0.1 and grown to an OD_{600} 0.5–1.0. Tenfold serial dilutions were spotted onto minimal medium for plate assays. The plates were cultured for 3 d, and the colonies representing living cells were counted for comparisons. The hexose transporter deletion strain EBY.VW4000 was transformed with SGB1 and grown on SD medium (ura dropout) containing 2% glucose for 4 d.

For sugar sensitivity, assays were performed essentially as described by Arenas-Huertero *et al*. (2000). Sterilized, dry seeds were sown on 1/2 MS medium supplemented with 0–7% D-glucose. Seedlings were grown for 10 d in constant dim light, and the numbers of green plants were scored.

Xenopus Oocyte Expression and Glucose Uptake Assays, SGB1 Antiserum

Construction of plasmids pHW136 through 139 is described in Supplemental Table S3. The plasmid containing the constitutively active human glucose transporter pGLUTX1(LL-AA) construct, to generate RNA for oocyte injection, was obtained from Dr. Mary Carayannopoulos (Washington University, St. Louis, MO). This plasmid harbors mutations in the GLUT coding region, which change LL amino acids to AA, causing the loss of insulin dependence for high-level glucose transport. Plasmids were linearized using EcoRI for pHW137 and pHW139, SacI for pHW137, and SalI for pGLUTX1 (LL-AA). Stage V–VI oocytes were injected with 50 ng of RNA prepared from *SGB1* sense and antisense, respectively, and hmGLUTX1 (LL-AA) cDNA. 2-Deoxy-D-glucose (2-DOG) uptake assays were conducted 3 d after injection of oocytes as described by Ibberson *et al*. (2000), except the amount of injected RNA in the present study was doubled. Briefly, the oocyte cells were incubated with 2 mM 2-DOG and 10 μCi of [1,2-^{3}H]deoxy-D-glucose (Sigma-Aldrich, St. Louis, MO) in a volume of 0.5 ml at 23°C for 50 min. 2-DOG uptake remains linear at 45 min. Cells were washed, lysed, and the radioactivity was measured by scintillation counting.

Antiserum against the SGB1 peptide MRGRHIDKRVPSKEFLSALC conjugated to keyhole limpet hemocyanin was generated in rabbits. The antiserum (#661) was used at a dilution of 1:5000 for immunoblot analyses.

RESULTS

Screen for Dominant Extragenic Alleles that Suppress agb1-2 Phenotypes

To identify new components required in G protein signaling in plants, we screened ~20,000 T1 seedlings for dominant extragenic alleles (Weigel *et al*., 2000) that suppress the etiolated hypocotyl and hook phenotypes of the Gβ null mutant *agb1-2* (Figure 1). Eight independent suppressor candidates, designated here as *sgb-1^D*-*8^D* for *S*uppressor of *G B*eta, were found to display, to different degrees, both an elongated hypocotyl and a closed hook after 2 d in darkness relative to *agb1-2*. One of these, *sgb-1^D*, is the subject of this study. As shown in Figure 1, A and B, the short hypocotyl of *agb1-2* at 2 d was partially suppressed in the hemizygous *sgb1-1^D*/homozygous *agb1-2* background, whereas the *agb1-2* hook phenotype was completely suppressed (Figure 1C).

In addition, the larger rosette size of *agb1-2* was also suppressed (Figure 1D) but other *agb1-2* phenotypes such as leaf shape (Figure 1F) were only partially suppressed, and others such as silique shape (our unpublished data) were not suppressed at all by the *sgb1-1^D* mutation.

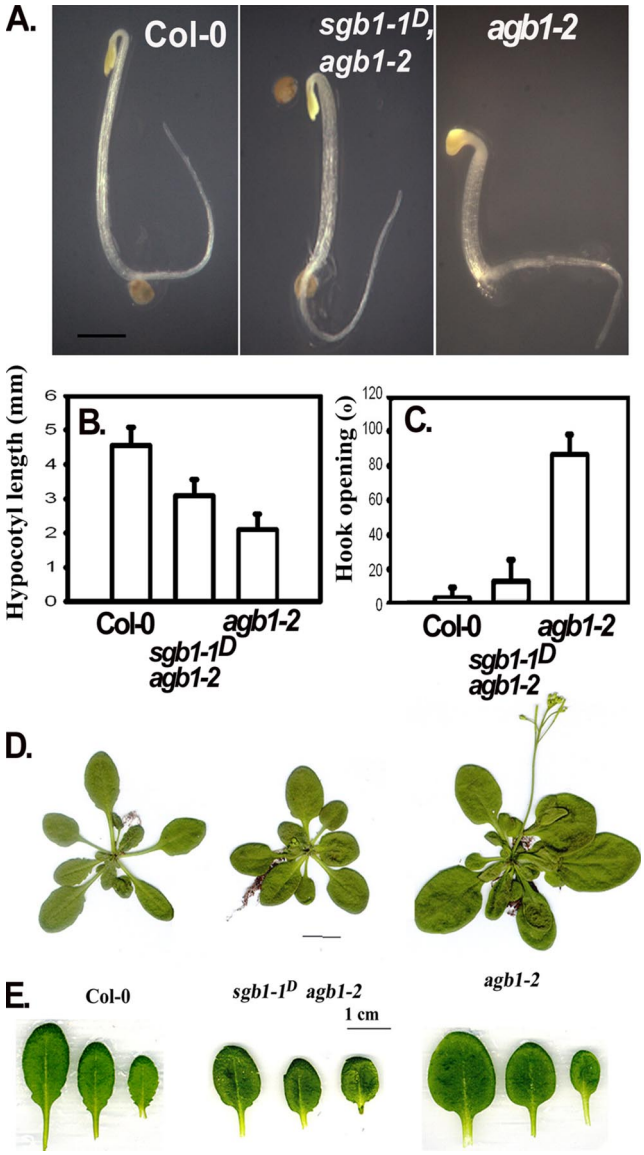

Figure 1. *sgb1-1^D* restores some *agb1-2* (Gβ) mutant phenotypes to wild type. (A) Two-day-old etiolated seedlings with the indicated genotype. Wild type Col-0 has a long hypocotyl and closed hook, the parental Gβ loss-of-function mutant *agb1-2* has a short hypocotyl and opened hook. The suppressor mutant *sgb1-1^D*, generated in the mutant *agb1-2* background fully and partially restored the *agb1-2* hook phenotype and hypocotyl phenotypes, respectively. Bar, 1 mm. A minimum of 10 seedlings were used to determine the mean of the hypocotyl length (B) and hook angle degree (C) and corresponding SE of the mean. (D) Rosette size of mature *sgb1-1^D*/*agb1-2* plants is restored to wild-type, whereas leaf shape and serration (E) is (T2) partially restored. Bar, 1 cm.

Suppressor of G Beta

The *sgb1-1^D agb1-2* line contained a single copy T-DNA insertion located at position 30,032,723 of chromosome 1, ~1 kb 5′ to the start codon of At1g79820. Four genes were found within a 20-kb region flanking the insertion (Figure 2A). Therefore, to identify which gene was activated, the steady-state mRNA levels of these four adjacent genes were analyzed using RT-PCR. Only At1g79820 showed an enhanced steady-state mRNA level compared with the parent *agb1-2* (Figure 2A).

To confirm that the dominant suppressor phenotypes was a consequence of overexpression at this locus, the full-length cDNA encoded by the At1g79820 locus was placed under the control of the cauliflower mosaic viral 35S promoter and transformed into the parent *agb1-2* mutant. Hypocotyl and hook phenotypes of *agb1-2* mutant were restored to wild type in three independent transgenic lines overexpressing the At1g79820 cDNA in *agb1-2* (Figure 2, B and C, lines 1–3, and D). The D-glucose hypersensitivity of *agb1-2* hypocotyls was also rescued when At1g79820 was overexpressed (Fig-

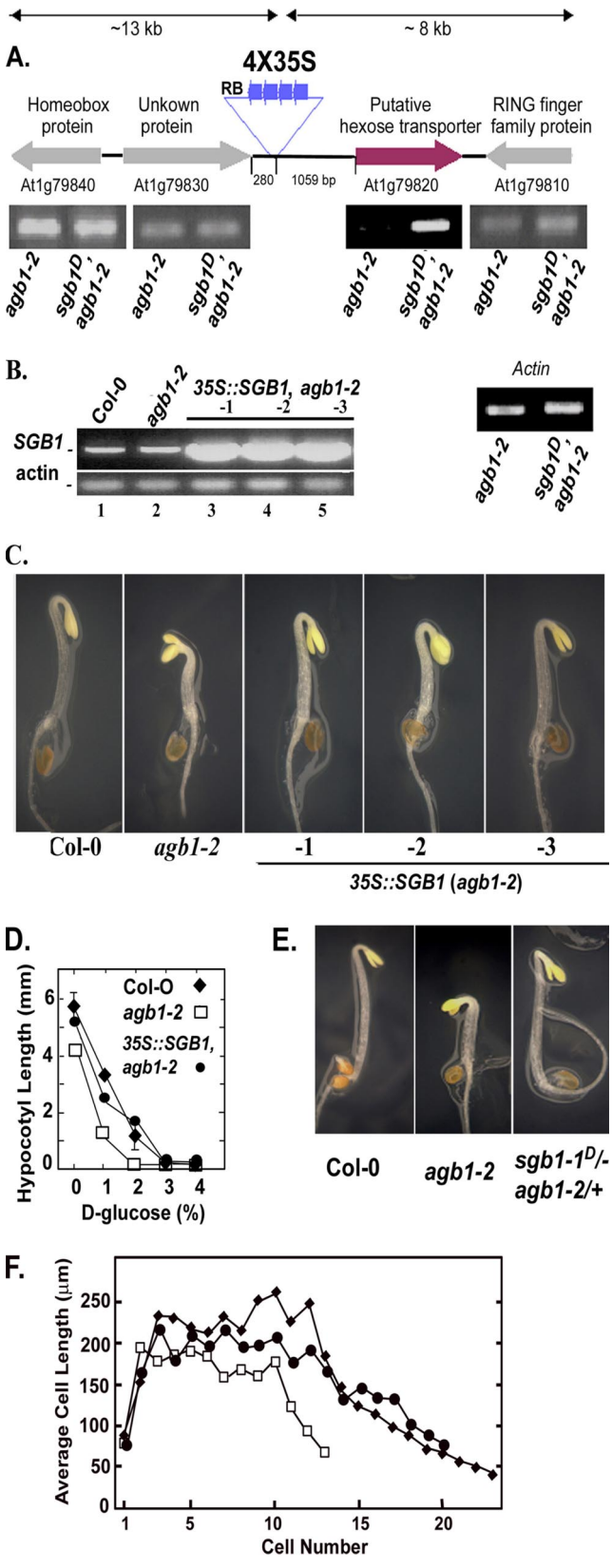

Figure 2. Identification of the *SGB1* locus and recapitulation of the *sgb1-1^D* mutant phenotype. (A) The insertion site of a tandem 4X 35S enhancer element in the *sgb1-1^D/agb-2 mutant* plant (T1) was determined by plasmid rescue. The relative steady-state transcript levels of four genes flanking the T-DNA insert (~10-kb length each side) were estimated by semiquantitative PCR using RNA from 2-wk-old rosette leaves (constant light; 22°C) of *agb1-2* single and the *sgb1-1^D agb-2* double mutants. An elevated steady-state RNA level was found for locus At1g79820, a putative hexose transporter in *Arabidopsis*. Longer PCR cycling revealed an At1g79820 band in *agb1-2*. The *β-actin* 2 gene served as the normalization control. (B) The steady-state At1g79820 RNA levels in plants harboring a transgene driven by the constitutive 35S promoter-driven were measured by RT-PCR in three independent transformed lines in the *agb1-2* genotype (lanes 3–5, lines 1→3). Shown for comparison are the steady-state At1g79820 RNA levels in the Col-0 wild-type and *agb1-2* genotypes. (C) Recapitulation of the wild-type phenotype in the *agb1-2* mutant was performed using 2-d-old seedlings grown in dark. *Arabidopsis* (*agb1-2*) was transformed with a 35S CaMV viral promoter driving the expression of the *SGB1* cDNA (pHW101). Lines 1→3 mimicked the phenotype of the suppressor *sgb1–1^D agb1*-2 with partially elongated hypocotyl and closed hooks. (D) Quantitation of hypocotyl lengths as a function of D-glucose is shown for wild type (solid diamonds), *agb1-2* expressing SGB1 (closed circles), and *agb1-2* (open squares). The data are from one experiment repeated twice with the same results. (E) *sgb1–1^D/−* (hemizygous), *agb-2/+* (heterozygous) did not display additional phenotypes. (F) Ectopic expression of *SGB1* (35S::SGB1) in *agb1-2* has increased cell numbers in developing hypocotyls. ◆, Col-0; □, *agb1-2*; ●, *35S:SGB1,agb1-2*. The number and length of epidermal cells of the hypocotyl were determined as described in *Materials and Methods*. Cell number begins with the basal cell at the root–shoot junction and increases apically toward the hook of the 2-d-old etiolated seedling. The average of the SEM for cell length measurement was ±26 μm.

ure 2D). These results support our conclusion that enhanced expression of At1g79820 causes suppression of the *agb1* phenotypes in *sgb1-1^D agb1-2* and based on these, we designate At1g79820 as *SGB1*. Seedlings that were hemizygous for the *SGB1-1^D* locus and heterozygous for the *agb1-2* allele (i.e., Agb1$^+$) exhibited the wild-type phenotype (Figure 2E). Because *agb1/+*, *sgb1-1^D* seedlings behaved similarly to wild-type seedlings, this result suggests that *sgb1-1^D* only affects hypocotyl and hook formation in the *agb1-2* loss-of-function background. Consistent with this observation, overexpression of the *SGB1* cDNA (35S::SGB1) in wild-type seedlings did not confer an obvious phenotype in these assays, nor did it alter morphology or development of adult plants (our unpublished data).

The underlying cause for restoration of the short hypocotyls of *agb1-2* seedlings to wild-type hypocotyl lengths when expression of *SGB1* is elevated is due to an increase in cell number (Figure 2F). There were on average 23 cells along a file on the hypocotyl epidermis of wild-type seedlings in contrast to 12 cells for *agb1-2* hypocotyls similar to values published by Ullah *et al*. (2003). Seedlings expressing *SGB1* under the 35S promoter have files comprised of 20 cells. The maximum and minimum cell lengths for all three genotypes are similar, indicating that the cell division defect occurring during early development in *agb1-2* is restored by SGB1.

Taken together, the dependence of a loss of AGB1 for a phenotype when *SGB1* is overexpressed suggests that *SGB1* lies on the same genetic pathway as *AGB1*. It also suggests that AGB1 acts as a positive regulator of SGB1.

SGB1 Encodes a Putative Hexose Transporter

The SGB1 protein, composed of 495 amino acids, has a predicted molecular mass of 52.4 kDa and an isoelectric point of ≈9 for an unphosphorylated form and 6 for a predicted fully phosphorylated form. The majority of protein topology servers (http://aramemnon.botanik.unikoeln.de) return a prediction for SGB1 having 10–12 transmembrane (TM) domains (Figure 3A, overlying dark lines), a

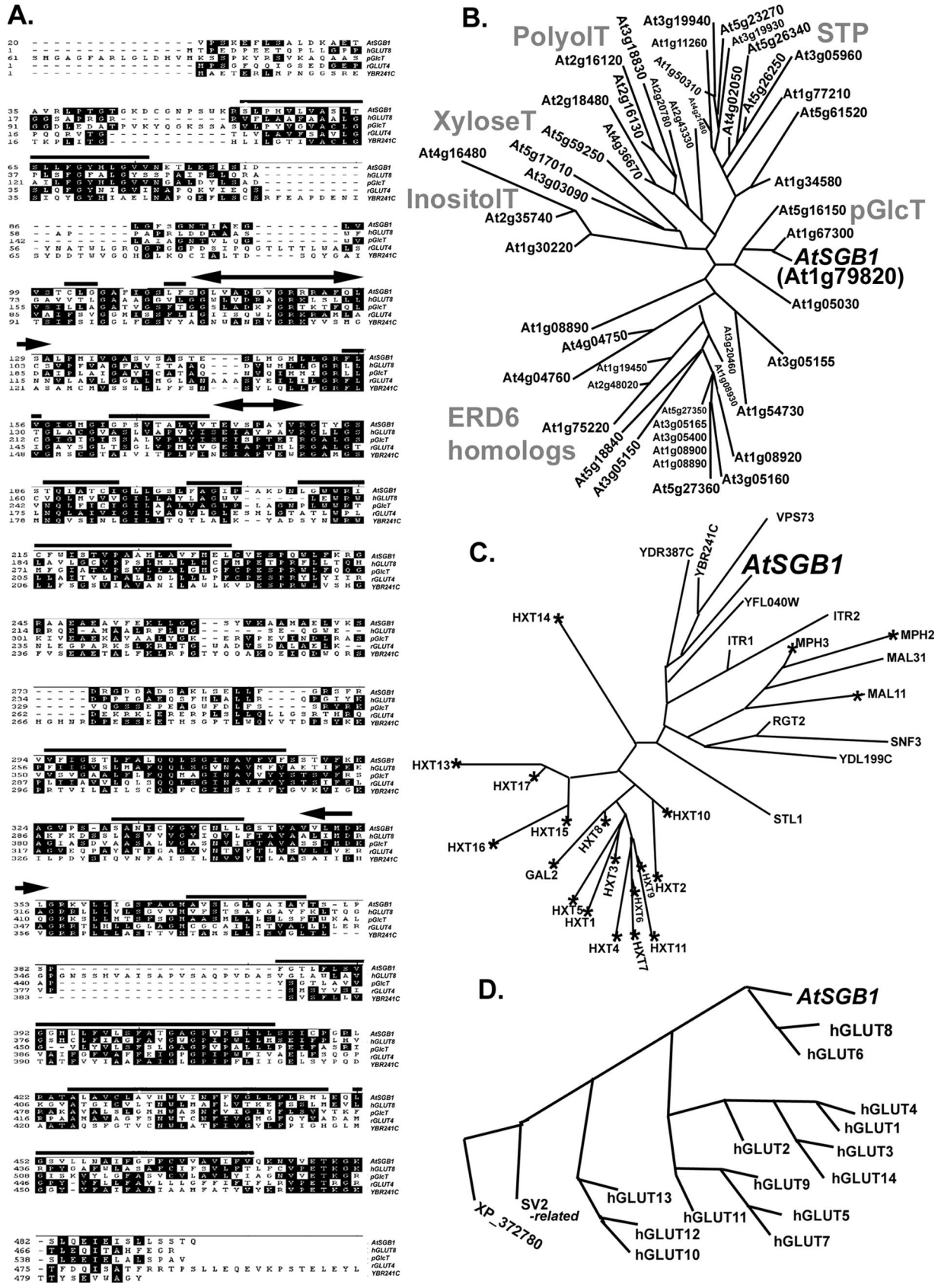

Figure 3. The architecture of SGB1, a putative hexose transporter and a comparison to yeast and vertebrate homologues. (A) The *SGB1* open reading frame encodes 495 amino acids. Partial sequences of SGB1 (At1g79820), a putative plastidic glucose transporter (pGlcT, At5g16150), and a rat glucose transporter 4 (GLUT4, NP_036883), and full-length sequences of human glucose transporter 8 (GLUT8, NP_055395 and an

central cytosolic loop and N- and C-terminal internal domains, and two sugar transport signatures (Figure 3A, double-arrow lines). A 12-TM topology is typical of sugar transporters in human, yeast, and plants (Marger and Saier, 1993; Buttner and Sauer, 2000; Wood and Trayhurn, 2003). SGB1 is most similar to a plastidic glucose transporter in plants (46% identical, 66% similar), to the human glucose transporter GLUT8 (28% identical, 48% similar), and to YBR241C, a putative transporter in budding yeast (28% identical, 48% similar).

SGB1 belongs to a large superfamily of known and putative hexose transporters with at least 50 members in *Arabidopsis* (Figure 3B). This superfamily, designated monosaccharide-H+ transporter-like (MST-like) proteins (http://www.biologie.uni-erlangen.de/mpp/TPer/index_TP.shtml), is one of the largest gene families in *Arabidopsis*, with most members having unknown functionality. The exceptions are the known sugar transporters (STP1-14, STP clade; Figure 3B) that have essential function throughout plant development (Sauer *et al*., 1990; Truernit *et al*., 1996, 1999; Sherson *et al*., 2000; Schneidereit *et al*., 2003, 2005; Scholz-Starke *et al*., 2003). The large family of *Arabidopsis* MST-like proteins is composed of several clades. One large clade (STP) is composed of known and putative glucose transporters. Other clades contain putative inositol transporters, anion transporters, polyol transporters, and glucose transporters. SGB1 (At1g79820) is a member of the plastidic glucose transporter clade (pGlcT) composed of four uncharacterized proteins and is annotated as such solely on protein similarities to a spinach plastid glucose translocator (Weber *et al*., 2000). Only one member of pGlcT (At5g16150) has a predicted chloroplast transit peptide (ChloroP = 0.83). SGB1 has a higher probability for mitochondrial targeting (TargetP:mtSP = 0.48) than for chloroplast targeting (ChloroP = 0.23), but neither prediction score strongly supports a mitochondrial or plastidic subcellular location.

SGB1 is similar to putative and known hexose transporters in yeast and humans. Yeast has 32 sugar transporters that fall into three major clades (Figure 3C). A comparison of *Arabidopsis* SGB1 (AtSGB1, Figure 3) to the *Saccharomyces cerevisiae* protein database with a cut-off E value of 4.8×10^{-10} places AtSGB1 among a group of unknown proteins, and it is most closely related to YBR241C and VPS73. Cladistic analyses using a cluster model places SGB1 within the 16 most similar glucose transporters in humans (cut-off E value of 8×10^{-11}). Human GLUT8 is the most similar to AtSGB1 (Figure 3, A and D).

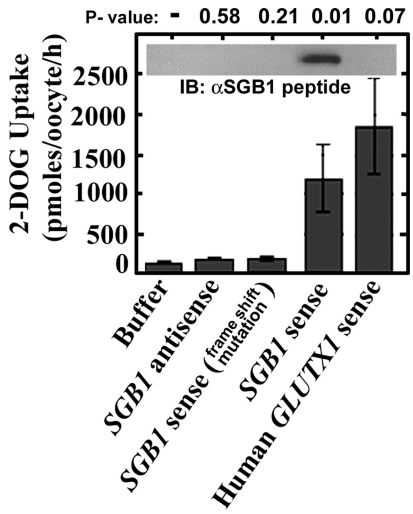

Figure 4. Deoxyglucose transport. Glucose uptake in oocyte cells overexpressing *Arabidopsis* SGB1 protein. The indicated RNA (50 ng) was injected into oocyte cells. Glucose uptake was carried out on the third day as described in *Materials and Methods*. Two negative controls were antisense *SGB1* RNA and a frame-shifted mutant RNA of SGB1, which introduces a premature stop codon. The positive control was a constitutively active human glucose transporter designated GLUTX1′LL-AA. The inset shows the immunoblot analysis of oocyte extracts probed with serum directed against SGB1 as described in *Materials and Methods*.

SGB1 Transports 2-Deoxy D-Glucose

Heterologous expression in oocytes in conjunction with 2-DOG uptake assays support the predicted hexose transport activity of SGB1. The oocyte assay is a well established in vivo assay system for heterologous hexose transport (Gould *et al*., 1991). Expression levels of SGB1 in oocytes after mRNA injection was demonstrated by immunoblot analysis using antisera directed to a 19-amino acid peptide located near the amino terminus of SGB1, which is predicted to be surface exposed and extracellular. SGB1 was detected in oocytes injected with sense mRNA but not the negative or positive controls (Figure 4, inset). Two negative controls were incorporated. As shown in Figure 4, [^{3}H]2-

Figure 3 (cont). unknown protein from yeast (YBR241C) are aligned using DNA STAR Mega alignment. Regions of SGB1 with high probability to be membrane spanning are indicated by bold horizontal lines. A transmembrane domain hidden Markov model was used for transmembrane prediction. Sugar transporter signature 1 and 2 predicted for SGB1 are indicated by the double-headed arrows. The N-terminal extensions of SGB1 and pGlcT are truncated as is the C-terminal extension on rGLUT4 for space consideration. (B) SGB1 is a member of the monosaccharide transporter (-like) family. There are 49 proteins shown to be similar to SGB1 above a cut-off of 4×10^{-16} for *Arabidopsis*. These were analyzed cladistically as described in *Materials and Methods*. The family is composed of six clades of which functionality has either been determined experimentally for at least one submember or inferred bioinformatically. *Arabidopsis* SGB1 (designated in this figure as *AtSGB1* for cross-genome comparison) is a member of a small group of plastidic glucose transporters. Although none of the *Arabidopsis* pGlcT have been shown experimentally to transport a monosaccharide, a pGlcT from spinach having high similarity to AtSGB1 has experimental proof (Weber *et al*., 2000). Other clades are designated accordingly (http://www.biologie.uni-erlangen.de/mpp/TPer/index_TP.shtml): STPs are sugar transpoters. ERD6 homologues are the early responsive to dehydration stress proteins. PolyolT, XyloseT, and InositolT are transporters of polyol, xylose, and inositol transporters, respectively. (C) Among 31 expressed yeast hexose transporters and glucose sensors having sequence identity to AtSGB1 (cut-off E value = 4.8×10^{-10}), AtSGB1 is most similar to a subgroup of proteins with unknown function. The largest group is the hexose transporter family of *S. cerevisiae*, composed of 18 proteins (Hxt1–17, Gal2). These proteins and other three maltose transporters (MPH2, MPH3, and MAL11) are essential for metabolic glucose consumption. RGT2 and SNF3 are glucose sensors that generate an intracellular signal inducing expression of glucose transporter (HXT) genes (Ozcan and Johnston, 1999). A hexose transport deficient strain (EBY.VW4000) was generated through deletions in the 21 genes marked with an asterisk and used for genetic complementation by SGB1. Accession numbers for the yeast homologues are provided in the following Web site with GBS1 protein sequence as a query: http://seq.yeastgenome.org/cgi-bin/nph-blast2sgd. (D) Comparison of *Arabidopsis* SGB1-16 human hexose transporters. The E value cut-off for selecting the vertebrate sequences was 8×10^{-11}. Accession numbers for the human homologues are provided in the following Web site with GBS1 protein sequence as a query: http://www.ncbi.nlm.nih.gov/blast/Blast.cgi.

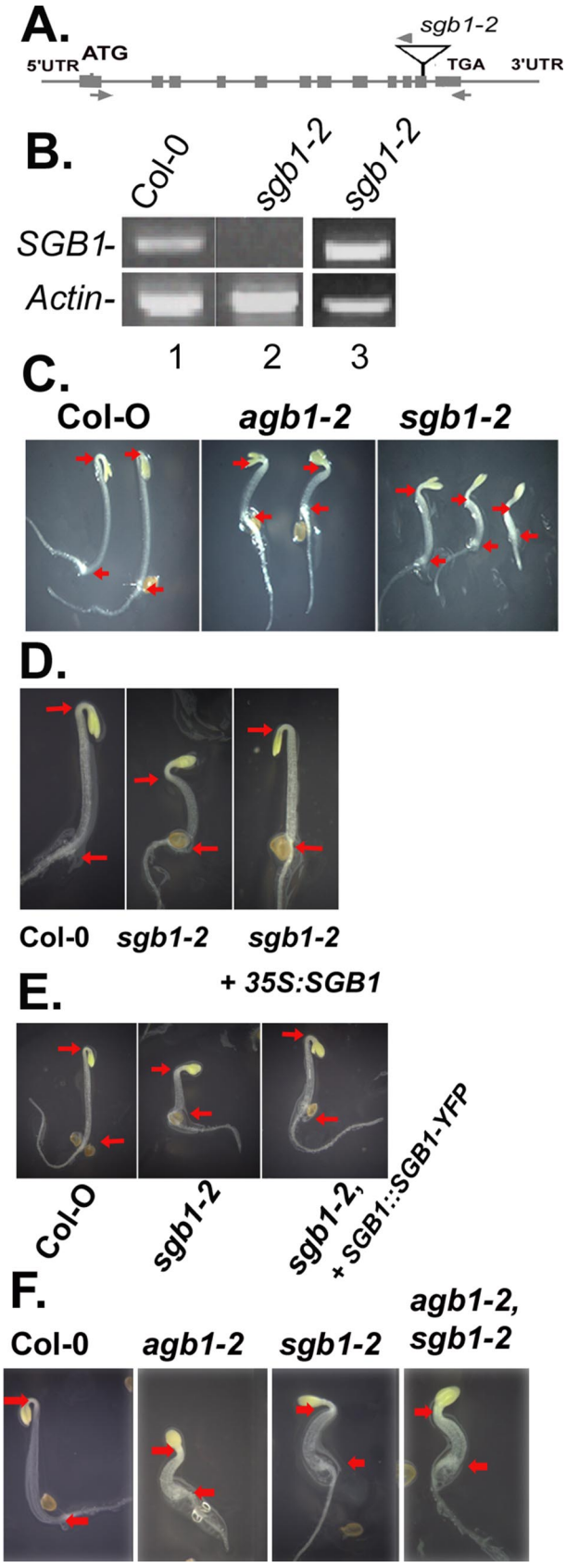

Figure 5. *SGB1* recessive mutants have overlapping phenotypes to *agb1-2*. (A) The *sgb1-2* allele contains a T-DNA insertion in the *SGB1* gene in the penultimate exon (T-DNA insert not drawn to scale). Arrows represent position of gene primers and arrowheads are T-DNA right border primers. (B) *SGB1* mRNA was analyzed in young leaves by using RT-PCR as described in *Materials and Methods*. Lanes 1 and 2 represent RT-PCR using the 5′ and 3′ *SGB1* primers (arrows). Lane 3 shows the RT-PCR product using the 5′ gene primer (left arrow) and the RB primer (arrowhead, Supplemental Table S1). Actin 2 primers in the same reactions were used for normalization (product = 0.9 kb). The *SGB1* PCR product is 1.5 kb. The *sgb1-2* PCR product is 1.6 kb. (C) *sgb1-2* showed similar morphology to *agb1-2* with shorter hypocotyls and open hooks. Red arrows mark the positions of the root–shoot transition zone (left arrow) and hook apex (right arrow), respectively, for hypocotyl length comparison. Seedlings were grown on 1/2 MS medium in dark for 2 d. (D) The *sgb1-2* mutant was genetically complemented with a 35S driven *SGB1* cDNA (D) or a *SGB1* promoter-driven SGB1-YFP translational fusion cDNA (E). (F) The *agb1-2 sgb1-2*, double mutant showed similar 2 d-phenotypes as the parents with open hook and short hypocotyl; no additive or synergistic phenotypes were observed.

DOG uptake into oocytes injected with antisense *SGB1* RNA and *SGB1* RNA containing a frame-shift mutation were not significantly different from oocytes injected with buffer alone and were at values similar to the nontransport controls reported by Ibberson *et al*. (2000) on a per oocyte basis. In contrast, *SGB1* sense RNA resulted in 10-fold greater transport than controls and at values similar to the positive control, injection of a constitutively active glucose transporter 1 (Ibberson *et al*., 2000).

Complementation analysis with *SGB1* tested with several yeast single and multiple deletion mutations (Supplemental Table S2) in known and putative hexose transporters (Figure 3C) was performed. However, despite extensive effort, rescue of either strong or weak phenotypes of hexose transporter null lines was not convincing (our unpublished data).

SGB1 Recessive Mutants Mimic agb1-2 Etiolated Phenotypes

A T-DNA-insertion mutant allele of locus At1g79820, designated here as *sgb1-2* in the Col-0 ecotype was isolated from the Salk Institute sequence-indexed insertion mutant collection (Alonso *et al*., 2003). The T-DNA insertion is located in the highly conserved region of the penultimate exon (Figure 5A). Semiquantitative PCR revealed the absence of full-length *SGB1* transcript, although a truncated transcript was detectable (Figure 5B). Neither the absence nor excessive amount of SGB1 had an effect on *AGB1* gene expression (Supplemental Figure S2). The transcript levels of genes encoding the other known G protein elements, GCR1 (Pandey and Assmann, 2004), GPA1 (Ullah *et al*., 2001), RGS1 (Chen *et al*., 2003), or the GPA1-interacting protein THF1 (Huang *et al*., 2006) were not changed by altered expression of SGB1 (Supplemental Figure S2).

Similar to the *agb1-2* mutant, 2-d-old etiolated *sgb1-2* seedlings exhibited short hypocotyls and open hooks (Figure 5C). The *sgb1-2* allele conferred phenotypes that behaved recessively (our unpublished data). To confirm that the mutant phenotypes were caused by the T-DNA insertion at the *SGB1* locus, we genetically complemented *sgb1-2* mutant plants. Transgenic *sgb1-2* plants expressing *SGB1* (Figure 5D), or the fusions *SGB1-YFP* or *SGB1-GUS* (our unpublished data), displayed wild-type phenotypes. The observation that the *sgb1-2* mutant had deficiencies in early development similar to the *agb1-2* mutant suggests an associate role of SGB1 with AGB1 in cell division and elongation. Moreover, similar morphological phenotypes implicate SGB1 and AGB1 in the same pathway of G protein signaling, consistent with the results from the *sgb1-1*^{D} gain-of-function

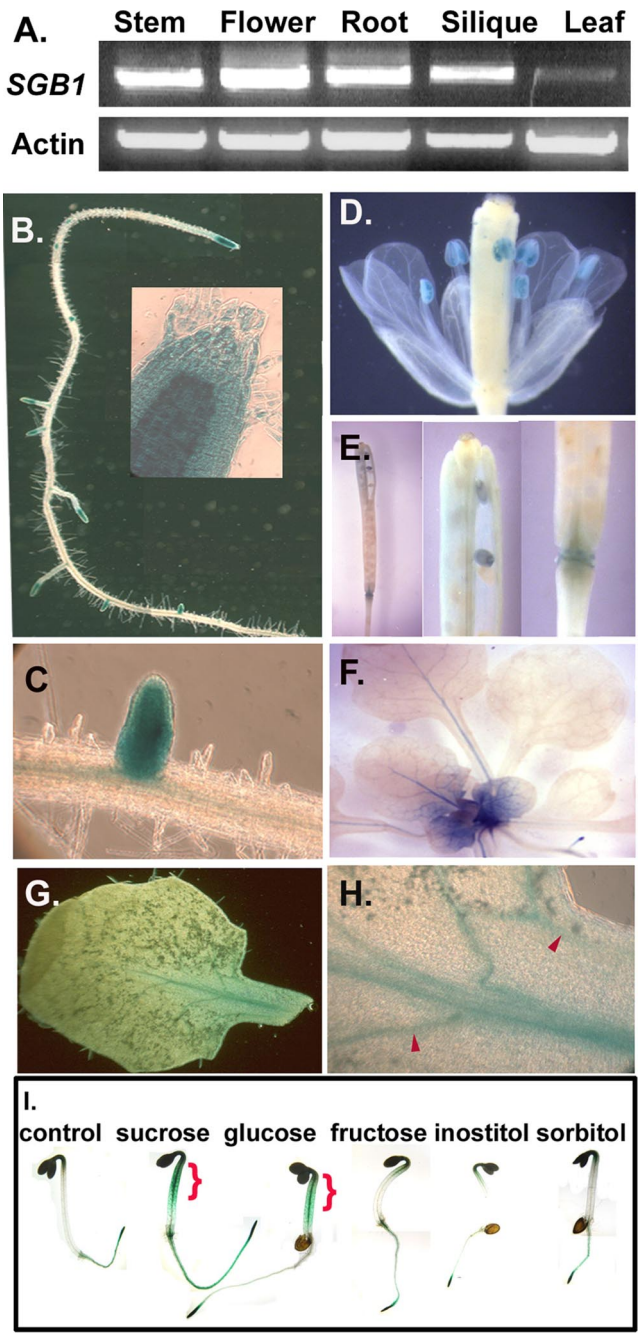

Figure 6. Steady-state levels of SGB1 protein are highest in sink tissues. (A) RT PCR using primers amplifying the full-length 1.5-kb *SGB1* cDNA (Figure 5A, arrows), generated from total RNA isolated from the indicated organs. "Leaf" means young leaves only. The *β-actin 2* level was used for normalization. (B–H). Transgenic Col-0 plants expressing a SGB1-translational GUS fusion protein driven by the *SGB1* promoter (pHW130) are stained for β-glucoronidase activity as described in *Materials and Methods*. (B) Fifteen-day-old root with apical root meristem shown as inset (C) Lateral root. (D) Flower showing anther and pollen staining. (E) Silique showing abscission zone staining (left and right), seed staining (center). (F) Newly divided cells of young leaves of 15-d-old light-grown plants; SGB1-GUS was detectable only in sink/young leaves rather in source/mature leaves. (G) Young leaf. (H) Vascular cells of a young leaf. Mature leaves lacked any detectable GUS activity. At least three lines were analyzed with the representative results shown here. (I). Glucose is a trigger for *SGB1* expression in hypocotyls and hooks. Two-day-old transgenic seedlings, bearing the native promoter-driven SGB1-GUS were used to monitor SGB1 responses to sugars. Seeds of transgenic plants bearing *pSGB1:*SGB1-GUS were grown on 1/2 MS medium supplemented with 0 or 1% glucose, sucrose, sorbitol, inositol, or fructose. Two-day-old etiolated seedlings were stained for GUS activity as described in *Materials and Methods*. Glucose and sucrose increased the steady-state levels of *SGB1* in hypocotyls, hooks, and the entire roots.

mutants. To test the genetic relationship further, epistasis analysis was performed between the *agb1-2* and *sgb1-2* alleles. The 2-d-old seedlings of the *agb1-2 sgb1-2* double mutant grown on 1% sucrose showed a similar phenotype to *agb1-2* or *sgb1-2* with short hypocotyls and open hooks (Figure 5F); neither an additive nor synergistic phenotype was observed.

Together, the recessive *sgb1-2* phenotype and the epistasis between loss-of-function alleles of *agb1* and *sgb1-2* suggests that AGB1 acts as a positive regulator of SGB1 in the early seedling development.

SGB1 Protein Is Predominantly Expressed in Tissues with Active Cell Division

SGB1 RNA was detected in various tissues of wild-type plants by RT-PCR (Figure 6A). Consistent with these RT-PCR results, an analysis of gene expression profiling data deposited in the GENEVESTIGATOR database (https://www.genevestigator.ethz.ch) showed that *SGB1* mRNA was detectable in a wide range of tissues. No single treatment or tissue type tested to date in the public database displayed altered *SGB1* RNA levels over controls or average by more than two-fold. Of particular interest, D-glucose altered *SGB1* expression only 1.3-fold (Genevestigator, version September 2005). Therefore, to elucidate the differences in steady-state levels of SGB1 protein in various cells due to possible posttranslational control, we transformed both *agb1-2* and Col-0 with a construct containing the *SGB1* promoter driving the *SGB1* cDNA translationally fused with the *GUS* gene. Overexpression of SGB1-GUS in the *agb1-2* mutant conferred wild-type hypocotyl length and hook angle, indicating that the SGB1-GUS fusion protein is active (our unpublished data). High steady-state levels of SGB1 protein were observed for various sink tissues both in the presence (wild-type Col-0) and absence (*agb1-2*) of AGB1 protein. The apical and lateral root meristems (Figure 6, B and C), displayed high SGB1 levels. SGB1 protein was also high in anthers/pollen (Figure 6D), embryos, and specific cells of the siliques, including the abscission zone of the floral organs (Figure 6E). Dividing, but not mature, leaf cells contained high SGB1 levels (cf. Figure 6, F and G). A specific set of newly formed cells of vascular traces in expanding leaves was shown to contain SGB1 (Figure 6H, arrowheads). The SGB1-GUS pattern greatly overlaps the *AGB1* expression pattern (Ullah *et al*., 2003).

Because SGB1 may function in AGB1-dependent sugar sensing (Figures 2D and S1) and because most signal networks contain feedback regulation, the effect of D-glucose on SGB1 protein level in planta was tested using an SGB1-GUS translational fusion driven by the *SGB1* promoter (Figure 6I). Etiolated seedlings grown without sugars express SGB1 in root meristems. Application of D-glucose greatly increased the steady-state level of the SGB1-GUS fusion protein and its distribution pattern. The D-glucose-induced increase was observed predominantly in the hypocotyl and root apices (Figure 6I, brackets). Similarly, sucrose increased the steady-state level of SGB1-GUS but with less efficacy. Sorbitol, inositol, and fructose did not alter the levels or distribution pattern of SGB1 over the no-sugar control.

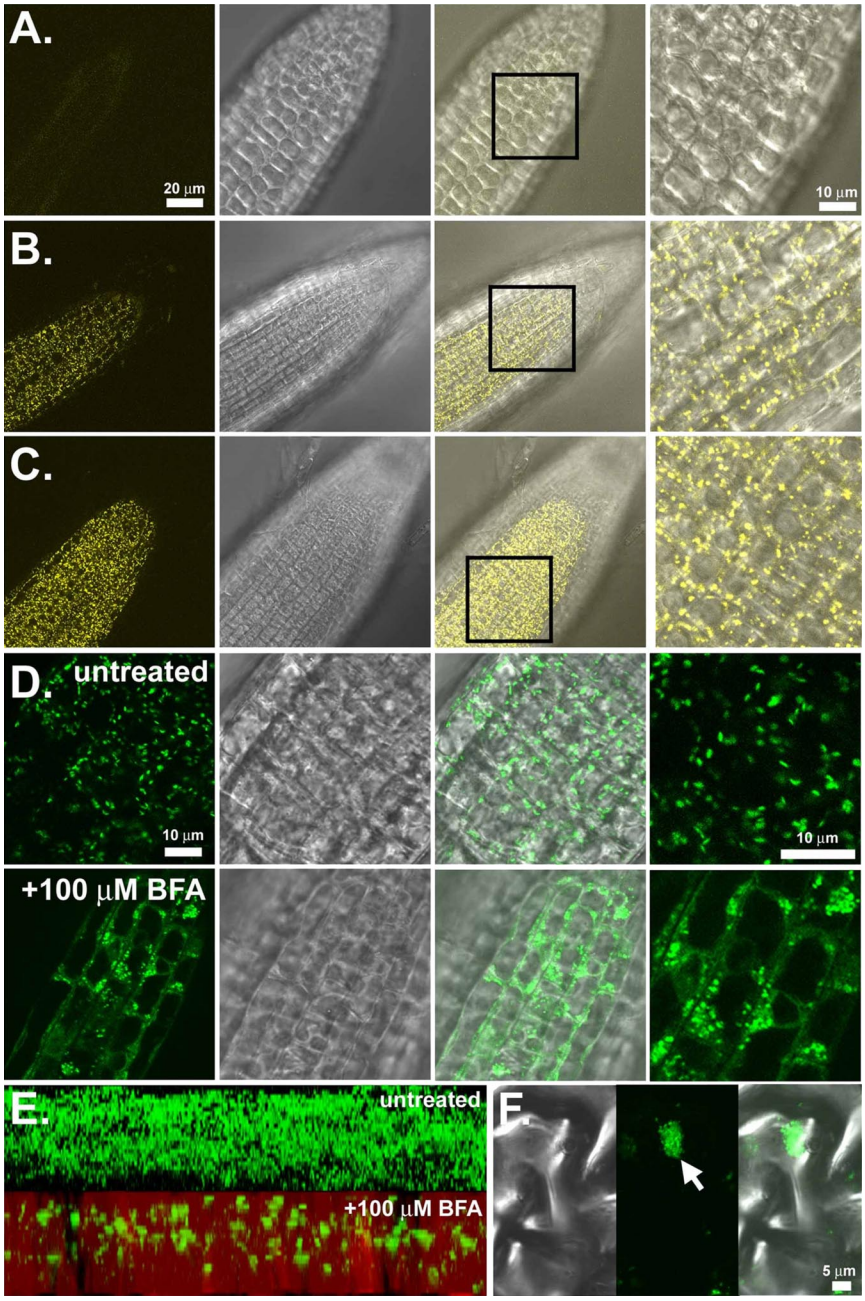

Figure 7. SGB1 is localized to the Golgi apparatus. (A) Wild type (Col-0) roots. (B) Imaging of *SGB1* promoter-driven *SGB1-YFP* in the wild-type background. Individual Golgi stacks are seen as punctuate structures rapidly moving throughout the cytosol. (C) Imaging of native promoter driven SGB1-YFP in the *agb1-2* background. (D) SGB1-GFP localization is sensitive to brefeldin-A (BFA). GFP imaging of the 35S promoter-driven SGB1-GFP before (untreated) and after (+100 μM BFA) treatment with BFA for 90 min, demonstrating the change in localization. (E) Z-stack reconstruction of *35S::SGB1-GFP* expression in leaf tissues before (above) and after (below) 100 mM BFA treatment. (F) High-magnification imaging of a single BFA compartment in a leaf epidermal cell expressing SGB1-GFP. Left, DIC; middle, fluorescence; and right, merge.

SGB1 *Is a Golgi-localized Protein*

Arabidopsis plants expressing an SGB1-YFP translational fusion driven by the *SGB1* promoter enabled the determination of the subcellular localization of SGB1 (Figure 5E). We first experimentally ruled out the predicted (in silico) mitochondrial and/or plastidic localizations of SGB1. Root tip cells of transgenic plants bearing *pSGB1::*SGB1-cyan fluorescent protein (*CFP*) and counterstained with MitoTracker, a mitochondrion-specific fluorescent dye (Invitrogen), revealed that mitochondrial fluorescence did not colocalize with SGB1-CFP fluorescence (our unpublished data). In addition, chloroplast-containing mesophyll cells expressing an SGB1:: GFP fusion protein, reveal no overlap between chlorophyll and GFP (our unpublished data).

SGB1-YFP driven by the native promoter in wild-type (Figure 7B) and *agb1-2* null (Figure 7C) backgrounds showed that fluorescence was observed in root tissues where the *SGB1* promoter is active (Figure 6, B and C). Moreover, the fluorescence imaging was observed to be in multiple punctate compartments within each cell, reminiscent of the size, distribution, and number of Golgi apparatus in plant cells (Boevink *et al.*, 1998). Moreover, the dynamics of SGB1-GFP movement (our unpublished data) also matched published Golgi dynamics (http://www.bio.utk.edu/cellbiol/iv/default.htm). Imaging a *pSGB1*::SGB1-YFP fluorescent construct in plants lacking functional AGB1 (Figure 7B) demonstrated that the localization of SGB1 was not dependent on AGB1 as the fluorescence patterns in Figure 7, B and C, are identical. Finally, because the SGB1 steady-state levels are higher in hypocotyl cells when grown on 1% D-glucose (Figure 6I), we examined hypocotyl epidermal cells and found the same punctate pattern for SGB1-YFP localization as in root cells (our unpublished data).

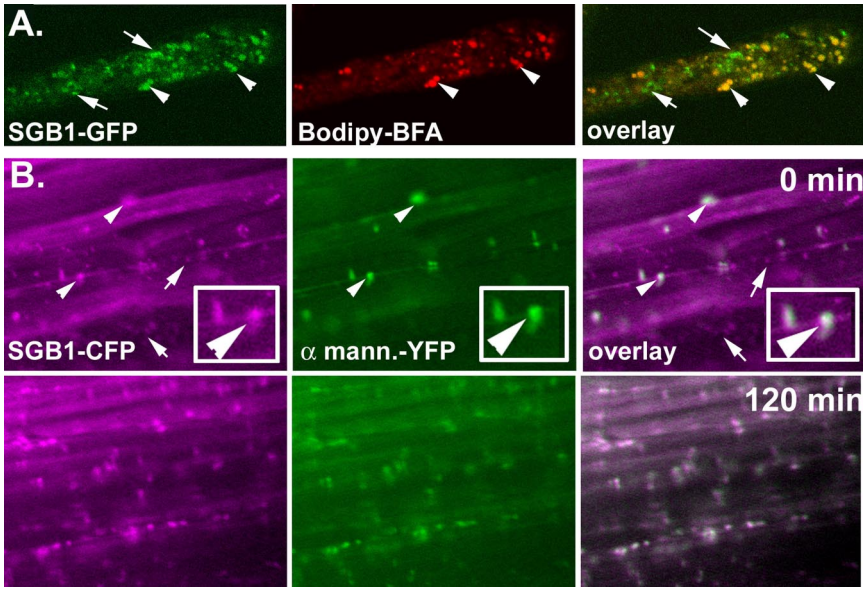

Figure 8. SGB1 is trafficked via Golgi and other vesicles. (A) Imaging of Bodipy-BFA–labeled root hair cells in *Arabidopsis* plants expressing *SGB1-GFP* driven by the CaMV 35S viral promoter. Left, localization of SGB1. SGB1 displayed predominant but not exclusive localization to the Golgi Apparatus (middle and right, see arrowheads). However, SGB1 is also found in small vesicles (arrows). (B) Hypocotyl cells of *Arabidopsis* plants expressing SGB1-CFP (left, false colored magenta) driven by the native *SGB1* promoter and the *cis*-medial Golgi marker α-mannosidase-YFP (α-mann.-YFP, middle, false colored green). Right, merged images where white represents overlap of signals. Addition of 1% D-glucose caused the reduction of SGB1 localization in the rapidly cycling smaller vesicles with a commensurate increase in SGB1 within the Golgi (arrows and Supplemental Movies S1–3).

To confirm that the observed fluorescence was the Golgi apparatus, BFA was used. BFA has been shown in plants to disrupt the integrity of Golgi stacks, resulting in the fusion of the endoplasmic reticulum (ER) and the Golgi stacks and the formation of so called "BFA compartments" (Ritzenthaler *et al*., 2002). After treatment with brefeldin-A (Figure 7D, bottom), the GFP fluorescence was observed to change from punctate structures representing the Golgi to both a diffuse fluorescence representing the fused ER/Golgi compartments and larger punctate structures representing the newly formed BFA compartments (Ritzenthaler *et al*., 2002).

Z-stack reconstruction imaging of the young leaf epidermal cells of SGB1-GFP plants before (Figure 7E, untreated) and after BFA treatment (Figure 7D, +100 μM BFA) clearly demonstrate the effect of BFA on SGB1 localization. Higher magnification imaging of an individual BFA compartment (Figure 7, F and G) demonstrated that the larger BFA compartments were made up of fused smaller compartments, presumably individual Golgi stacks. Figure 7F is a three-dimensional reconstruction from a Z-stack acquisition of control and BFA-treated cells.

Bodipy-BFA has been previously shown to label the Golgi complex in living cells (Deng *et al*., 1995). We used Bodipy-BFA to stain Golgi in *Arabidopsis* seedlings expressing SGB1-GFP driven by the cauliflower mosaic virus (CaMV) 35S promoter. In *Arabidopsis* root hair cells, SGB1-GFP showed a predominant colocalization with Bodipy-BFA–labeled Golgi stacks that were dispersed in the cytoplasm (Figure 8A, arrowheads). Under these conditions, SGB1-GFP protein was also associated with vesicles typically smaller than the Golgi stacks and that did not stain with Bodipy-BFA (Figure 8A, arrow). To further elucidate the localization of SGB1 and to understand the nature of the small non-Golgi vesicles, we used *Arabidopsis* seedlings expressing both SGB1-CFP driven by the *SGB1* promoter and the *cis*-medial Golgi marker α-mannosidase-YFP driven by the CaMV 35S promoter. As shown using the Bodipy-BFA Golgi reporter (Figure 8A), SGB1-CFP was observed in Golgi as well as within rapidly moving small vesicles (Figure 8B and Supplemental Movies S1–3). Interestingly, the addition of 1% D-glucose caused within minutes a decrease in the smaller SGB1-CFP–labeled vesicles (Figure 8B, arrow, and Supplemental Movies S1–3). As can be seen in Figure 8B (bottom), nearly all the SGB1-CFP fluorescence colocalizes with the Golgi marker after a low concentration of D-glucose was applied. This redistribution was most apparent in the supplemental movies where the rates of movement of the smaller vesicles and the SGB1-CFP–labeled Golgi were perceptively different. Concomitant and commensurate with the D-glucose–induced decrease in the number of small vesicles containing SGB1-CFP, the SGB1-labeled Golgi compartments increased. This indicates that the Golgi is the predominant SGB1 compartment and further suggests that D-glucose regulates the SGB1 trafficking between the Golgi and as yet unidentified small vesicle compartments.

In summary, four lines of evidence indicate that the predominant but not exclusive subcellular localization of SGB1 is the Golgi apparatus: 1) the SGB1 compartment share the size, morphology, and dynamics of plant Golgi; 2) BFA reversibly causes the SGB1-GFP fluorescence pattern to collapse into diffuse ER/Golgi punctuate structures and the previously described BFA compartment derived from the Golgi; 3) SGB1 colocalizes with the Golgi stain Bodipy-BFA; and 4) SGB1 colocalizes with the *cis*-medial Golgi enzyme α mannosidase. Moreover, we have shown that SGB1 is found to various degrees, depending on the conditions, in smaller rapidly moving vesicles and that the addition of D-glucose diminishes their abundance in the cortical region of the plant cell.

DISCUSSION

In metazoans, the Gβγ dimer regulates the activity of phospholipase Cβ, adenyl cyclase (AC), and G protein-coupled inwardly rectifying potassium channel potassium channels; however, *Arabidopsis* lacks these candidate effectors. Therefore, without directly testable hypotheses for Gβγ activation of plant targets, we sought to define novel candidate plant effectors that are positively regulated by the *Arabidopsis* Gβ subunit, AGB1, and/or downstream elements in the Gβγ signal network. Our approach used activation tagging in a Gβ-null genotype with the rationale that overexpression of Gβγ targets would compensate for the loss of AGB1 activation. Although activation tagging has been useful as a forward genetic tool to dissect roles for genes in large families, only recently has it become useful to identify genetic sup-

pressors in *Arabidopsis* (Li *et al*., 2002). The emphasis in the present study is suppression by a dominant allele of a hexose transporter gene of etiolated hypocotyl length conferred by loss of AGB1.

One of the high D-glucose sensing pathways in yeast uses a Gα subunit (GPA2) to activate AC and ultimately protein kinase A (Lemaire *et al*., 2004). Evidence suggests that the activated form of *Arabidopsis* GPA1 is also involved in sugar sensing because *rgs1* mutants (Chen *et al*., 2003, 2006b; Chen and Jones, 2004) and GTPase-deficient GPA1 mutants (Huang *et al*., 2006) are D-glucose tolerant, whereas *gpa1* null mutants are hypersensitive to D-glucose (Ullah *et al*., 2002). However, this does not involve AC activation, and a direct role for the Gβγ subunit has not been demonstrated. We have shown that *agb1-2* mutants are severely hypersensitive to applied D-glucose (Supplemental Figure S1), suggesting that either the Gβγ dimer is required for Gα recruitment/action or that the Gβγ dimer plays a direct role in sugar signal transduction. The latter possibility is favored because D-glucose hypersensitivity in the *agb1* mutant (Supplemental Figure S1) is much greater than observed for the *gpa1* mutants. The greater D-glucose hypersensitivity of the *agb1* mutants makes the *agb1-2* genotype more suitable for a robust suppressor screen and thus was our rationale for the selection of *agb1* over *gpa1* mutants.

Upon receptor activation, the released Gβγ dimer modulates the activities of effectors in concert or opposition to the activated Gα subunit. This action is nearly always constrained to the plasma membrane, although there are a few examples of Gβγ localization at a subcellular membrane (Brunk *et al*., 1999). Because Gβγ is predominantly found at the plasma membrane and SGB1 is in the Golgi, the genetic interaction between Gβγ and SGB1 is indirect biochemically. The most likely mechanism involves a secondary messenger whose production is initiated at the plasma membrane but has a site of action distally, possibly on SGB1.

We have shown that overexpression of a Golgi-localized hexose transporter is able to restore some phenotypes that result from the loss of AGB1. This suggests that the action or subcellular translocation of SGB1 is a consequence of AGB1 function or a subset of AGB1-mediated signaling networks. There is a role for a mammalian heterotrimeric G protein in the translocation of glucose transporters, although the mechanism is unconventional, and the Gα subtype remains controversial (Patel, 2004; Dugani and Klip, 2005). Nonetheless, these studies raise the possibility of D-glucose regulation of SGB1 translocation in *Arabidopsis* and point to future experimentation.

The purpose for D-glucose signaling in plants remains to be elucidated, but it has been suggested that D-glucose controls energy carbon homeostasis (Zhou *et al*., 1998; Sheen *et al*., 1999; Xiao *et al*., 2000; Leon and Sheen, 2003; Gibson, 2005) as is known for mammals. We propose here an additional possibility, namely, that external D-glucose may signal growth strategies in plants as is well known for yeast (Versele *et al*., 2001; Tamaki *et al*., 2005). Specifically, we hypothesize that D-glucose, a recognized regulator of cell cycle gene expression in plants (discussed above) and yeast (Vanoni *et al*., 2005), together with AGB1, already shown to be involved in cell proliferation (Ullah *et al*., 2003), operate on the same pathway to modulate cell proliferation rates in apical and intercalary meristems. It is most likely that there are many targets to the heterotrimeric G protein complex subunits, each resulting in the control of some aspect of cell proliferation such as control of the nuclear cycle and cell wall synthesis. A role for a Golgi-localized hexose transporter is a likely control element for the latter.

The mechanism of sugar sensing in plants may be unique (Sheen *et al*., 1999; Gibson, 2005); however, as in yeast, downstream from sugar perception lie controls for plant cell proliferation through the stability of cyclins, other cell cycle regulators (Riou-Khamlichi *et al*., 2000; Menges and Murray, 2002; Lorenz *et al*., 2003; Planchais *et al*., 2004), and transcription (Thum *et al*., 2004). Exogenous sugar, especially D-glucose, has profound effects on *Arabidopsis* development, and many of these are known to involve light perception by the phytochrome photoreceptor. For example, in the etiolated seedling, sugars and phytochrome regulate hypocotyl length and hook angle (Misera *et al*., 1994; Short, 1999; Ullah *et al*., 2002; Takahashi *et al*., 2003; Laxmi *et al*., 2004). During and after de-etiolation, sugar and light regulate cotyledon expansion, hypocotyl growth, anthocyanin level, and lignin biosynthesis (Dijkwel *et al*., 1997; Borisjuk *et al*., 1998; Salchert *et al*., 1998; Rogers *et al*., 2005).

The concentration of extracellular D-glucose in plants is unknown. It is therefore difficult to evaluate whether applications of D-glucose above 3%, as shown in Supplemental Figure S1 and in published work (Arenas-Huertero *et al*., 2000), are physiologically relevant or instead induce a neomorphic response through, for example, a stress mechanism. Extremely high D-glucose levels (molar) are found in tissues such as in fruit, but the levels of extracellular D-glucose in different tissues have yet to be determined. The role for high glucose in signaling is an extraordinarily complicated problem to solve, because it must take into consideration that D-glucose is rapidly taken up, a high concentration of sucrose occurs in apoplastic transport and must encounter localized invertases within their cell walls, cells may have desensitization mechanisms operating as a function of concentration and exposure time, and there are no physiological assays for D-glucose responses with response times in minutes to assess this (current sugar sensitivity assays are in days using organ growth acclimated in applied glucose concentrations). In vivo extracellular sensors for D-glucose (Deuschle *et al*., 2005) are required to answer unequivocally this question, but these are not yet available. However, indirect measurements have been applied to address this problem, and estimates of apoplastic levels of D-glucose at 150 mM (3%) or higher have been suggested (McLaughlin and Boyer, 2004; Makela *et al*., 2005). For example, sorghum embryos develop in as high as 6% apoplastic D-glucose (Maness and McBee, 1986).

Nonetheless, could the suppression by *sgb1-1*^{D} be a means to counter the inability to cope with a glucose stress conferred by the loss of AGB1? Although not to be ruled out, two lines of evidence do not support this. First, the etiolated phenotype rescued by *sgb1-1*^{D} and by the overexpression of *SGB1* is apparent under normal physiological conditions (i.e., 1% D-glucose or sucrose; Figures 1 and 2). Second, the increased SGB1 expression does not confer a sugar phenotype when this hypothetical stress is relieved (Figure 2E).

How can increased hexose transport into the Golgi rescue hypocotyl length in the *agb1-2* mutant and what is a possible mechanism for AGB1 action? Hypocotyl growth occurs by cell expansion from a limited set of cells laid down during embryogenesis. *agb1-2* hypocotyls have a reduced number of cells; consequently, the hypocotyl length is reduced (Ullah *et al*., 2003). During mitosis, plants build a wall through the secretion and translocation of membrane and wall materials. This type of wall formation requires de novo wall synthesis of which some components are assembled in the Golgi, most notably the pectins and xyloglucans (Munoz *et al*., 1996; Baydoun *et al*., 2001). One possible explanation is that wall synthesis is increased as a consequence of elevated

glucose in the Golgi. Pectins and xyloglucans are internalized in root cells and subsequently are deposited into the nascent cell plate during division (Baluska *et al*., 2005). As discussed above, sugars control the rate of cell division by multiple means from control of cell cycle machinery to wall synthesis. Thus, one of the modes of action of AGB1 may be to control glucose transport into the Golgi directly or indirectly through SGB1, which consequently affects division wall synthesis.

In conclusion, although several hexose transporters have to date been characterized, SGB1 represents the first in the unknown pGlcT clade and the first in plants shown to be localized to the Golgi apparatus. SGB1 and AGB1 are found in tissues with high cell division activity. Most importantly, SGB1 and AGB1 genetically operate in the pathway, extending the current evidence that a heterotrimeric G protein complex plays a role in modulating cell proliferation in *Arabidopsis*.

ACKNOWLEDGMENTS

We thank Dr. Jin-Gui Chen for generating the screening populations, Jing Yang for experimental assistance, Dr. Mary Carayannopoulos for the hGLUTX1 plasmid, the Salk Institute Genomic Analysis Laboratory and *Arabidopsis* Stock Center for the T-DNA line materials, and Dr. Boles for the yeast strain EBY.VW4000. We also greatly appreciate helpful discussions with Drs. N. Allen, P. Morgan, and Z. Chen. Work in A.M.J.'s laboratory on the *Arabidopsis* G protein is supported by National Institute of General Medical Sciences Grant GM-65989-01, Department of Energy Grant DE-FG02-05ER15671, and National Science Foundation Grant MCB-0209711.

REFERENCES

Aharon, G. S., Snedden, W. A., and Blumwald, E. (1998). Activation of a plant plasma membrane Ca^{2+} channel by TGα1, a heterotrimeric G protein α-subunit homologue. FEBS Lett. *424*, 17–21.

Alonso, J. M., *et al*. (2003). Genome-wide insertional mutagenesis of *Arabidopsis thaliana*. Science *301*, 653–657.

Arenas-Huertero, F., Arroyo, A., Zhou, L., Sheen, J., and Leon, P. (2000). Analysis of *Arabidopsis* glucose insensitive mutants, gin5 and gin6, reveal a central role of the plant hormone ABA in the regulation of plant vegetative development by sugar. Genes Dev. *14*, 2085–2096.

Baluska, F., Liners, F., Hlavacka, A., Schlicht, M., Van Cutsem, P., McCurdy, D. W., and Menzel, D. (2005). Cell wall pectins and xyloglucans are internalized into dividing root cells and accumulate within cell plates during cytokinesis. Protoplasma *225*, 141–155.

Baydoun, E.A.-H., Abdel-Massih, R. M., Dani, D., Riszk, S. E., and Brett, C. T. (2001). Galactosyl- and fructosyltransferases in etiolated pea epicotyls: product identification and subcellular localization. J. Plant Physiol. *158*, 145–150.

Bechtold, N., Ellis, J., and Pelletier, G. (1993). In planta *Agrobacterium* mediated gene transfer by infiltration of adult *Arabidopsis thaliana* plants. C.R. Acad. Sci. Paris *316*, 1194–1199.

Boevink, P., Oparka, K., Santa Cruz, S., Martin, B., Betteridge, A., and Hawes, C. (1998). Stacks on tracks: the plant Golgi apparatus traffics on an actin/ER network. Plant J. *15*, 441–447.

Borisjuk, L., Walenta, S., Weber, H., Mueller-Klieser, W., and Wobus, U. (1998). High resolution histographical mapping of glucose concentrations in developing cotyledons of *Vicia faba* in relation to mitotic activity and storage processes: glucose as a possible developmental trigger. Plant J. *15*, 583–591.

Brodsky, L. I., Ivanov, V. V., Ya, S., Kalaydzidis, A.M.L., Yu, S., Osipov, A. R., Tatuzov, L., and Feranchuk, S. I. (1992). GeneBee: the program package for biopolymer structure analysis. Dimacs *8*, 127–139.

Brodsky, L. I., Ivanov, V. V., Kalaydzidis, Y. L., Leontovich, A. M., Nikolaev, V. K., Feranchuk, S. I., and Drachev, V. A. (1995). GeneBee-NET: Internet-based server for analyzing biopolymers structure. Biochemistry *60*, 923–928.

Brunk, I., Pahner, I., Maier, U., Jenner, B., Veh, R. W., Nurnberg, B., and Ahnert-Hilger, G. (1999). Differential distribution of G-protein beta-subunits in brain: an immunocytochemical analysis. Eur J. Cell Biol. *78*, 311–322.

Buttner, M., and Sauer, M. (2000). Monosaccharide transporters in plants: structure, function and physiology. Biochim. Biophys. Acta *1465*, 263–272.

Chen, J.-G., Gao, Y., and Jones, A. M. (2006a). Differential roles of *Arabidopsis* heterotrimeric G-protein subunits in modulating cell division in roots. Plant Physiol. *141*, 887–897.

Chen, J.-G., and Jones, A. M. (2004). AtRGS1 function in *Arabidopsis thaliana*. Methods Enzymol. *389*, 338–350.

Chen, J.-G., Willard, F. S., Huang, J., Liang, J., Chasse, S. A., Jones, A. M., and Siderovski, D. P. (2003). A seven-transmembrane RGS protein that modulates plant cell proliferation. Science *301*, 1728–1731.

Chen, Y., Ji, F., Xie, H., Liang, J., and Zhang, J. (2006b). The regulator of G-protein signaling proteins involved in sugar and abscisic acid signaling in *Arabidopsis* seed germination. Plant Physiol. *140*, 302–310.

Csaszar, A., and Abel, T. (2001). Receptor polymorphisms and diseases. Eur. J. Pharmacol. *414*, 9–22.

Deng, Y., Bennink, J., Kang, H., Haugland, R., and Yewdell, J. (1995). Fluorescent conjugates of brefeldin A selectively stain the endoplasmic reticulum and Golgi complex of living cells. J. Histochem. Cytochem. *43*, 907–915.

Deuschle, K., Fehr, M., Hilpert, M., Lager, I., LalLonde, S., Looger, L. L., Okumoto, S., Persson, J., Schmidt, A., and Frommer, W. B. (2005). Genetically encoded sensors for metabolites. Cytometry *64A*, 3–9.

Dhanasekaran, N., Heasley, L. E., and Johnson, G. L. (1995). G protein-coupled receptor systems involved in cell growth and oncogenesis. Endocr. Rev. *16*, 16259–16270.

Dijkwel, P. P., Huijser, C., Weisbeek, P. J., Chua, N. H., and Smeekens, S. (1997). Sucrose control of phytochrome A signaling in *Arabidopsis*. Plant Cell *9*, 583–595.

Dohlman, H. G. (2002). G proteins and pheromone signaling. Annu. Rev. Physiol. *64*, 129–152.

Dugani, C. B., and Klip, A. (2005). Glucose transporter *4*, cycling, compartments and controversies. EMBO Rep. *6*, 1137–1142.

Gibson, S. I. (2005). Control of plant development and gene expression by sugar signaling. Curr. Opin. Plant Biol. *8*, 93–102.

Gould, G. W., Thomas, H. M., Jess, T. J., and Bell, G. I. (1991). Expression of human glucose transporters in *Xenopus* oocytes: kinetic characterization and substrate specificities of the erythrocyte, liver, and brain isoforms. Biochemistry *30*, 5139–5145.

Huang, J., Taylor, J. P., Chen, J.-G., Uhrig, J. F., Schnell, D. J., Nakagawa, T., Korth, K. L., and Jones, A. M. (2006). The plastid protein THYLAKOID FORMATION1 and the plasma membrane G-protein GPA1 interact in a novel sugar-signaling mechanism in *Arabidopsis*. Plant Cell *18*, 1226–1238.

Ibberson, M., Uldry, M., and Thorens, B. (2000). GLUTX1, a novel mammalian glucose transporter expressed in the central nervous system and insulin-sensitive tissues. J. Biol. Chem. *275*, 4607–4612.

Jones, A. M., and Assmann, S. M. (2004). Plants: the latest model system for G-protein research. EMBO Rep. *5*, 572–578.

Lapik, V. R., and Kaufman, L. S. (2003). The *Arabidopsis cupin* domain protein AtPirin1 interacts with the G protein α subunit GPA1 and regulates seed germination and early seedling development. Plant Cell *15*, 1578–1590.

Laxmi, A., Paul, L. K., Peters, J. L., and Khurana, J. P. (2004). *Arabidopsis* constitutive photomorphogenic mutant, bls1, displays altered brassinosteroid response and sugar sensitivity. Plant Mol. Biol. *56*, 185–201.

Lease, K. A., Wen, J., Li, J., Doke, J. T., Liscum, E., and Walker, J. C. (2001). A mutant *Arabidopsis* heterotrimeric G-protein β subunit affects leaf, flower, and fruit development. Plant Cell *13*, 2631–2641.

Lemaire, K., Van de Velde, S., Van Dijck, P., and Thevelein, J. M. (2004). Glucose and sucrose act as agonist and mannose as antagonist ligands of the G-protein coupled receptor Gpr1 in the yeast *Saccharomyces cerevisiae*. Mol. Cell *16*, 293–299.

Leon, P., and Sheen, J. (2003). Sugar and hormone connections. Trends Plant Sci. *8*, 110–116.

Li, J., Wen, J., Lease, K. A., Doke, J. T., Tax, F. E., and Walker, J. C. (2002). BAK1, an *Arabidopsis* LRR receptor-like protein kinase, interacts with BRI1 and modulates brassinosteroid signaling. Cell *110*, 213–222.

Lorenz, S., Tintelnot, S., Reski, R., and Decker, E. L. (2003). Cyclin D-knockout uncouples developmental progression from sugar availability. Plant Mol. Biol. *53*, 227–236.

Makela, P., McLaughlin, J. E., and Boyer, J. S. (2005). Imaging and quantifying carbohydrate transport to the developing ovaries of maize. Ann. Bot. *96*, 939–949.

Malamy, J., and Benfey, P. (1997). Organization and cell differentiation in lateral roots of *Arabidopsis thaliana*. Development *124*, 33–44.

Maness, N. O., and McBee, G. G. (1986). Role of placental sac endosperm carbohydrate import in sorghum caryopses. Crop Sci. *26*, 1201–1206.

Marger, M. D., and Saier, M.H.J. (1993). A major superfamily of transmembrane facilitators that catalyse uniport, symport and antiport. Trends Biochem. Sci. *18*, 13–20.

McLaughlin, J. E., and Boyer, J. S. (2004). Glucose localization in maize ovaries when kernel number decreases at low water potential and sucrose is fed to the stems. Ann. Bot. *94*, 75–86.

Menges, M., and Murray, J.A.H. (2002). Synchronous *Arabidopsis* suspension cultures for analysis of cell-cycle gene activity. Plant J. *30*, 203–212.

Misera, S., Muller, A. J., Weiland-Heidecker, U., and Jurgens, G. (1994). The FUSCA genes of *Arabidopsis*: negative regulators of light responses. Mol. Gen. Genet. *244*, 242–252.

Mishra, G., Zhang, W., Deng, F., Zhao, J., and Wang, X. (2006). A bifurcating pathway directs abscisic acid effects on stomatal closure and opening in *Arabidopsis*. Science *312*, 264–266.

Mumberg, D., Muller, R., and Funk, M. (1995). Yeast vectors for the controlled expression of heterologous proteins in different genetic backgrounds. Gene *156*, 119–122.

Munoz, P., Norambuena, L., and Orellana, A. (1996). Evidence for a UDP-glucose transporter in Golgi apparatus-derived vesicles from pea and its possible role in polysaccharide biosynthesis. Plant Physiol. *112*, 1585–1594.

Nielsen, H., Engelbrecht, J., Brunak, S., and von Heijne, G. (1997). Identification of prokaryotic and eukaryotic signal peptides and prediction of their cleavage sites. Protein Eng. *10*, 1–6.

Olof, E., Nielsen, H., Brunak, S., and von Heijne, G. (2000). Predicting subcellular localization of proteins based on their N-terminal amino acid sequence. J. Mol. Biol. *300*, 1005–1016.

Ozcan, S., and Johnston, M. (1999). Function and regulation of yeast hexose transporters. Microbiol. Mol. Biol. Rev. *63*, 554–569.

Pandey, S., and Assmann, S. M. (2004). The *Arabidopsis* putative G protein-coupled receptor GCR1 interacts with the G protein α subunit GPA1 and regulates abscisic acid signaling. Plant Cell *16*, 1616–1632.

Patel, T. B. (2004). Single transmembrane spanning heterotrimeric G protein-coupled receptors and their signaling cascades. Pharmacol. Rev. *56*, 371–385.

Planchais, S., Samland, A. K., and Murray, J.A.H. (2004). Differential stability of *Arabidopsis* D-type cyclins: CYCD3;1 is a highly unstable protein degraded by a proteasome-dependent mechanism. Plant J. *38*, 616–625.

Radhika, V., and Dhanasekaran, N. (2001). Transforming G proteins. Oncogene *20*, 1607–1614.

Riou-Khamlichi, C., Menges, M., Healy, J.M.S., and Murray, J.A.H. (2000). Sugar control of the plant cell cycle: differential regulation of *Arabidopsis* D-type cyclin gene expression. Mol. Cell. Biol. *20*, 4513–4521.

Ritzenthaler, C., Nebenfuhr, A., Movafeghi, A., Stussi-Garaud, C., Behnia, L., Pimpl, P., Staehelin, L. A., and Robinson, D. G. (2002). Reevaluation of the effects of brefeldin A on plant cells using Tobacco Bright Yellow 2 cells expressing Golgi-targeted green fluorescent protein and COPI antisera. Plant Cell *14*, 237–261.

Rockman, H. A., Koch, W. J., and Lefkowitz, R. J. (2002). Seven-transmembrane-spanning receptors and heart function. Nature *415*, 206–212.

Rogers, L. A., Dubos, C., Cullis, I. F., Surman, C., Poole, M., Willment, J., Mansfield, S. D., and Campbell, M. M. (2005). Light, the circadian clock, and sugar perception in the control of lignin biosynthesis. J. Exp. Bot. *56*, 1651–1663.

Rosenkilde, M. M., Waldhoer, M., Lüttichau, H. R., and Schwartz, T. W. (2001). Virally encoded 7TM receptors. Oncogene *20*, 1582–1593.

Sadee, W., Hoeg, E., Lucas, J., and Wang, D. (2001). Genetic variations in human G protein-coupled receptors: implications for drug therapy. AAPS PharmSci. *3*, 1–27.

Salchert, K., Bhalerao, R., Koncz-Kalman, Z., and Koncz, C. (1998). Control of cell elongation and stress responses by steroid hormones and carbon catabolic repression in plants. Philos. Trans. R. Soc. Lond. Ser. B *353*, 1517–1520.

Sànchez, R., and Marzluff, W. F. (2002). The Stem-loop binding protein is required for efficient translation of histone mRNA *in vivo* and *in vitro*. Mol. Cell. Biol. *22*, 7093–7104.

Sauer, N., Friedlander, K., and Graml-Wicke, U. (1990). Primary structure, genomic organization and heterologous expression of a glucose transporter from *Arabidopsis thaliana*. EMBO J. *9*, 3045–3050.

Schneidereit, A., Scholz-Starke, J., and Buttner, M. (2003). Functional characterization and expression analyses of the glucose-specific AtSTP9 monosaccharide transporter in pollen of *Arabidopsis*. Plant Physiol. *133*, 182–190.

Schneidereit, A., Scholz-Starke, J., Sauer, N., and Buttner, M. (2005). AtSTP11, a pollen tube-specific monosaccharide transporter in *Arabidopsis*. Planta *221*, 48–55.

Scholz-Starke, J., Buttner, M., and Sauer, N. (2003). AtSTP6, a new pollen-specific H+-monosaccharide symporter from *Arabidopsis*. Plant Physiol. *131*, 70–77.

Sheen, J., Zhou, L., and Jang, J.-C. (1999). Sugars as signaling molecules. Curr. Opin. Plant Biol. *2*, 410–418.

Sherson, S. M., Hemmann, G., Wallace, G., Forbes, S., Germain, V., Stadler, R., Bechtold, N., Sauer, N., and Smith, S. M. (2000). Monosaccharide/proton symporter AtSTP1 plays a major role in uptake and response of *Arabidopsis* seeds and seedlings to sugars. Plant J. *24*, 849–857.

Short, T. W. (1999). Overexpression of *Arabidopsis* phytochrome B inhibits phytochrome A function in the presence of sucrose. Plant Physiol. *119*, 1497–1506.

Takahashi, F., Sato-Nara, K., Kobayashi, K., Suzuki, M., and Suzuki, H. (2003). Sugar-induced adventitious roots in *Arabidopsis* seedlings. J. Plant Res. *116*, 83–91.

Tamaki, H., Yun, C.-W., Mizutani, T., Tsuzuki, T., Takagi, Y., Shinozaki, M., Kodama, Y., Shirahige, K., and Kumagai, H. (2005). Glucose-dependent cell size is regulated by a G protein-coupled receptor system in yeast *Saccharomyces cerevisiae*. Genes Cells *10*, 193–206.

Thum, K., Shin, M., Palenchar, P., Kouranov, A., and Coruzzi, G. (2004). Genome-wide investigation of light and carbon signaling interactions in *Arabidopsis*. Genome Biol. *5*, R10.

Truernit, E., Schmid, J., Epple, P., Illig, J., and Sauer, N. (1996). The sink-specific and stress-regulated *Arabidopsis* STP4 gene: enhanced expression of a gene encoding a monosaccharide transporter by wounding, elicitors, and pathogen challenge. Plant Cell *8*, 2169–2182.

Truernit, E., Stadler, R., Baier, K., and Sauer, N. (1999). A male gametophyte-specific monosaccharide transporter in *Arabidopsis*. Plant J. *17*, 191–201.

Ullah, H., Chen, J.-G., Temple, B., Boyes, D. C., Alonso, J. M., Davis, K. R., Ecker, J. R., and Jones, A. M. (2003). The β subunit of the *Arabidopsis* G protein negatively regulates auxin-induced cell division and affects multiple developmental processes. Plant Cell *15*, 393–409.

Ullah, H., Chen, J.-G., Wang, S., and Jones, A. M. (2002). Role of G protein in regulation of *Arabidopsis* seed germination. Plant Physiol. *129*, 897–907.

Ullah, H., Chen, J.-G., Young, J., Im, K.-H., Sussman, M. R., and Jones, A. M. (2001). Modulation of cell proliferation by heterotrimeric G protein in *Arabidopsis*. Science *292*, 2066–2069.

Vanoni, M., Rossi, R. L., Querin, L., Zinzalla, V., and Alberghina, L. (2005). Glucose modulation of cell size in yeast. Biochem. Soc. Trans. *33*, 294–296.

Versele, M., Lemaire, K., and Thevelein, J. M. (2001). Sex and sugar in yeast: two distinct GPCR systems. EMBO Rep. *21*, 574–579.

Wang, X.-Q., Ullah, H., Jones, A. M., and Assmann, S. M. (2001). G protein regulation of ion channels and abscisic acid signaling in *Arabidopsis* guard cells. Science *292*, 2070–2072.

Wang, Z.-F., Ingledue, T. C., Dominski, Z., Sanchez, R., and Marzluff, W. F. (1999). Two *Xenopus* proteins that bind the 3′ end of histone mRNA: implications for translational control of histone synthesis during oogenesis. Mol. Cell. Biol. *19*, 835–845.

Weber, A., Servaites, J. C., Geiger, D. R., Kofler, H., Hille, D., Groner, F., Hebbeker, U., and Flugge, U.-I. (2000). Identification, purification, and molecular cloning of a putative plastidic glucose translocator. Plant Cell *12*, 787–802.

Weigel, D., *et al*. (2000). Activation tagging in *Arabidopsis*. Plant Physiol. *122*, 1003–1013.

Wood, S., and Trayhurn, P. (2003). Glucose transporters (GLUT and SGLT): expanded families of sugar transport proteins. Br. J. Nutr. *89*, 3–9.

Xiao, W., Sheen, J., and Jang, J.-C. (2000). The role of hexokinase in plant sugar signal transduction and growth and development. Plant Mol. Biol. *44*, 451–461.

Zhou, L., Jang, J.-C., Jones, T. L., and Sheen, J. (1998). Glucose and ethylene signal transduction crosstalk revealed by an *Arabidopsis* glucose-insensitive mutant. Proc. Natl. Acad. Sci. USA *95*, 10294–10299.